Water Supply

IWA PUBLISHING

Water Supply Vol 22 No 1, 137 doi: 10.2166/ws.2021.281

Numerical and experimental study on solute transport through physical aquifer model

Muskan Mayank and Pramod Kumar Sharma*

Department of Civil Engineering, Indian Institute of Technology, Roorkee 247667, India
*Corresponding author. E-mail: pramod.sharma@ce.iitr.ac.in

ABSTRACT

Environmental concerns have drawn much research interest in solute transport through porous media. Thus, contaminants of groundwater permeate through pores in the ground, and adsorption attenuates the pollution concentration as the pollutants adhere to the solid surface. Mathematical models based on certain simplifying assumptions have been used to predict solute transport. The transport of solutes in porous media is governed by a partial differential equation known as the advection-dispersion equation. In this study, a two-dimensional numerical model has been developed for solute transport through porous media. Results of spatial moments have been predicted and analysed in the presence of both constant and time-dependent dispersion coefficients. Afterward, a numerical model is used to simulate experimentally observed breakthrough curves for both conservative and non-conservative solutes. Thus, transport parameters are estimated through numerical simulation of observed breakthrough curves. Finally, this model gives the best simulation of observed breakthrough curves, and it can also be used in the field scale.

Key words: breakthrough curves, numerical simulation, spatial moments, time dependent dispersion

HIGHLIGHTS

- Two-dimensional numerical model developed for advection-dispersion transport equation.
- Used constant, linear and asymptotic time dependent-dispersion coefficient.
- Simulation of spatial moments.
- Experimental breakthrough curves for conservative and non-conservative solutes.
- Simulation of observed breakthrough curves and estimated transport parameters.

INTRODUCTION

The hydrogeological properties of the subsurface zone are responsible for maintaining the quality of groundwater resources (Al Kuisi *et al.* 2009). Major processes such as advection, diffusion, dispersion, and sorption are accountable for deteriorating groundwater quality. The migration of dissolved contaminants in porous media is mainly controlled by advective transport through the fractures combined with the diffusion of solutes into the relatively immobile pore water in the soil matrix between fractures. The diffusion process, influencing both reactive and non-reactive tracers, can attenuate solute migration relative to the velocity of flow in the fractures and is often referred to as matrix diffusion (Chiogna *et al.* 2010). The attenuation of the solute particles due to chemical mixing depends on the nature of the sediment, the contaminant, and the geochemical environment (Belhachemi & Addoun 2011).

Analytical solutions of one-dimensional solute transport problems, subject to different initial and boundary conditions, infinite and the semi-finite domain have been reported by many researchers (Ogata & Banks 1961; Neville *et al.* 2000; Gao *et al.* 2010; Joshi *et al.* 2012; Leij *et al.* 2012; Sharma *et al.* 2015; Masciopinto & Passarella 2018). Solutions of two-, three-dimensional deterministic ADE's have been investigated in numerous studies and are still being actively studied (Freeze & Cherry 1979; Latinopoulos *et al.* 1988; Batu 1989; Leij *et al.* 1991, Batu 1993; Leij *et al.* 1993; Serrano 1995). A two-dimensional solute transport model for variably saturated porous media with different chemical ions has been investigated by Šimůnek & Suarez (1994). Early arrival and long tailing of breakthrough curves are observed for solute transport through heterogeneous porous media, which shows anomalous transport behaviour (Levy & Berkowitz 2003). Thus, the advection-dispersion equation with a constant dispersion model is less adequate for simulating anomalous transport through heterogeneous porous media. Hence, a time-dependent dispersion model is used to capture the anomalous transport

behaviour of a solute through saturated porous media (Huang *et al.* 1995; Gao *et al.* 2010). Marinoschi *et al.* (1999) explored a technique for the analytical solution of one-, two- and three-dimensional solute transport problems with time-dependent dispersion coefficients subjected to different boundary conditions. An analytical solution of a spatially variable coefficient advection-diffusion equation has been solved by Zoppou & Knight (1999) in up to three dimensions with the assumption that the velocity component is proportional to the distance and that the diffusion coefficient is proportional to the square of the corresponding velocity component. James & Jawitz (2007) have discussed a two-dimensional reactive transport ADE model using a splitting technique where advective, dispersive, and reactive parts of the equation were solved separately. An explicit finite-volume Godunov method was used to approximate the advective part, while a hybridized mixed finite element method was used to solve for the dispersive step and the backward Euler method for the reactive component.

Most of the researchers assumed that the dispersion coefficient is time-independent (Corey *et al.* 1970; Fenske 1979; Selvadurai 2004). Fried (1975) identified the scale effect of the dispersion coefficient due to temporal and spatial variability of the dispersion coefficient. Both field and laboratory-scale experiments show that in subsurface transport problems the dispersivity parameters can be considered as time-dependent (Fenske 1979). Stochastic analyses have shown that the dispersion may depend on travel time and may increase until it reaches an asymptotic value (Gelhar *et al.* 1979; Gelhar & Axness 1983). Analytical solutions of the solute transport equation considering time-dependent dispersion coefficients have been developed by Pickens & Grisak (1981), Yates (1992), and Barry & Sposito (1989). Yates (1990) obtained one-dimensional analytical solutions for uniform flow with boundary conditions of both constant concentration and constant flux type. Basha & El-Habel (1993) developed an analytical solution of the one-dimensional transport equation with time-dependent dispersion coefficients for an infinite domain. Aral & Liao (1996) derived a general analytical solution of the two-dimensional solute transport equation with time-dependent dispersion coefficients for an infinite domain aquifer.

The method of moment analysis is an important tool for computing mass recoveries in tracer experiments, travel velocities of the plume, and the description of the shape of the plume in terms of dispersivity, skewness, and kurtosis (Aris 1956). Thus, the method of the moment was employed for the study of many natural gradient field tracer tests (Freyberg 1986). The relationship between the spatial and temporal moments and the properties of an evolving solute plume is based on work by Aris (1956). Goltz & Roberts (1987) developed Aris's method of moments, which can be used to analyze the temporal and spatial moment behavior of concentration distributions obtained using both equilibrium and physical non-equilibrium solute transport models.

The spatial moments of the bromide tracer distribution were used to calculate the tracer mass, velocity, and dispersivity during the large-scale tracer test at the Canadian Air Force Base in Borden, Ontario (Freyberg 1986; Farrell *et al.* 1994). Knorr *et al.* (2016) performed a saturated dual-porosity soil column experiment and proposed a single fissure dispersion model, which includes the diffusive mass exchange between mobile and immobile water regions. Xu *et al.* (2019) reviewed the recent advancement in the context of experimental studies of dilution and reactive mixing in saturated porous media at steady-state conditions. Apiratikul (2020) studied the application of an analytical solution for the advection-dispersion reaction model to predict the three-dimensional plot of breakthrough curves and mass transfer for sorption of heavy metal ions using a fixed-bed column.

In this study, an attempt has been made to describe the two-dimensional advection-dispersion transport equation with time-dependent dispersion coefficients. A two-dimensional numerical model is developed using the implicit finite difference method. Also, experiments were conducted in the lab for solute transport through porous media consisting in the rectangular tank, and results of observed breakthrough curves were predicted for both conservative and non-conservative solutes.

GOVERNING EQUATIONS

Two-dimensional advective-dispersive transport equation considering equilibrium sorption can be written as (Aral & Liao 1996):

Deze vergelijking dus eens proberen dimensieloos te maken
=> Zie Technieken uit Hoofdstuk 2!

$$R\frac{\partial c}{\partial t} = D_L(t)\frac{\partial^2 c}{\partial x^2} + D_T(t)\frac{\partial^2 c}{\partial y^2} - v\frac{\partial c}{\partial x} \quad (1)$$

where $D_L(t)$ and $D_T(t)$ are time-dependent longitudinal and transverse hydrodynamic dispersion coefficients, v is the pore water velocity in x direction.

The expressions of longitudinal and transverse linear time-dependent dispersion coefficients can be written as (Aral & Liao 1996):

$$D_L(t) = D\frac{t}{C_L} + D_0 \tag{2a}$$

$$D_T(t) = 0.1D\frac{t}{C_L} + D_0 \tag{2b}$$

Based upon the stochastic theory, field observations, and numerical experiments, longitudinal asymptotic time-dependent dispersion coefficient can be described by Aral & Liao (1996):

$$D_L(t) = D_0 + D\frac{t}{(t + C_A)} \tag{3a}$$

Transverse asymptotic time-dependent dispersion coefficient can be written as (Anderson & Cherry 1979; Aral & Liao 1996):

$$D_T(t) = D_0 + 0.1D\frac{t}{(t + C_A)} \tag{3b}$$

Zie uitleg MT bodem!

where, D_0 is the sum of molecular diffusion and microdispersion (generally negligible), D is the macro dispersion coefficient at field scale, C_L represents linear time-dependent coefficient, and C_A indicates the asymptotic time-dependent coefficient.

FINITE DIFFERENCE METHOD

The Forward-time central-space (FTCS) method is a finite difference method used for numerically solving the heat equation and similar parabolic partial differential equations. It is a first-order method in time, explicit in time, and is conditionally stable when applied to the heat equation. When used as a method for advection equations, or more generally hyperbolic partial differential equations, it is unstable unless a retardation term is included (Dehghan 2004). The FTCS method is based on the central difference in space and the forward Euler method in time, giving first-order convergence in time and second-order convergence in space. Transport phenomenon is central for understanding many procedures in numerous sciences and is described by the partial differential equation.

Centered implicit finite difference technique has been used to formulate the numerical discretization of the governing transport Equation (1):

$$R\frac{C_{i,j}^{l+1} - C_{i,j}^{l}}{dt} = D_L(t)\left[\frac{C_{i+1,j}^{l+1} - 2C_{i,j}^{l+1} + C_{i-1,j}^{l+1}}{(dx)^2}\right] + D_T(t)\left[\frac{C_{i,j+1}^{l+1} - 2C_{i,j}^{l+1} + C_{i,j-1}^{l+1}}{(dy)^2}\right] - v\frac{C_{i+1,j}^{l+1} - C_{i-1,j}^{l+1}}{2\,dx} \tag{4}$$

where, l represents the known time label and $l+1$ represents the unknown time label.

Simplifying the above Equation (4) for concentration:

$$B_1C_{i,j}^{l+1} + B_2C_{i+1,j}^{l+1} + B_3C_{i-1,j}^{l+1} + B_4C_{i,j+1}^{l+1} + B_5C_{i,j-1}^{l+1} = RC_{i,j}^{l} \tag{5}$$

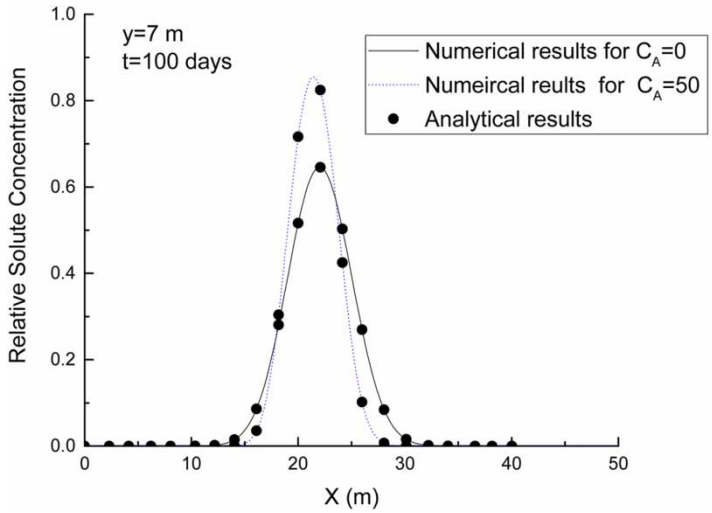

Figure 1 | Breakthrough curves for constant dispersion and asymptotic time-dependent dispersion models.

where,

$$B_1 = R + \frac{2\,\mathrm{D_L(t)}\,dt}{(dx)^2} + \frac{2\,\mathrm{D_T(t)}\,dt}{(dy)^2} \tag{6a}$$

$$B_2 = -\frac{\mathrm{D_L(t)}\,dt}{(dx)^2} + \frac{v\,dt}{2\,dx} \tag{6b}$$

$$B_3 = -\frac{\mathrm{D_L(t)}\,dt}{(dx)^2} - \frac{v\,dt}{2\,dx} \tag{6c}$$

$$B_4 = B_5 = -\frac{\mathrm{D_T(t)}\,dt}{(dy)^2} \tag{6d}$$

Hier dus zeker ook kijken naar alternatieven: ADI, L-mol, SOR

The Gauss-Seidel iteration method has been used to solve the set of linear simultaneous equations, and the convergence was found to be satisfactory for almost all cases. Both the Peclet number ($\mathrm{Pe} = v\,dx/\mathrm{D_L}$) and Courant number ($\mathrm{C_r} = v\,dt/dx$) are kept less than one to reduce the numerical error. Therefore, other iterative techniques, which may provide faster convergence, were not explored. The numerical model has been validated with an analytical solution Aral & Liao (1996), as shown in Figure 1. Following input parameters, pore water velocity $\mathrm{v} = 0.1$ m/day, longitudinal dispersion coefficient $\mathrm{D_L} = 0.035\ \mathrm{m^2/day}$, transverse dispersion coefficient $\mathrm{D_T} = 0.0035\ \mathrm{m^2/day}$, and injected plume size of 4.6 m × 5.6 m were used during simulation. The numerical results of breakthrough curves were predicted at $\mathrm{y} = 7$ m and flow direction in the x-axis. Value of asymptotic coefficient $\mathrm{C_A} = 0$ indicates a constant dispersion model, and $\mathrm{C_A} = 50$ day indicates an asymptotic dispersion model. Hence, the numerical model has validated both cases of constant and asymptotic time-dependent dispersion models.

Welke Deltax, deltay en deltat zijn gebruikt???

Geen toegang tot de paper zoals gebruikt voor de analytische benchmark

APPLICATIONS OF NUMERICAL MODEL

Simulation for spatial moments with an asymptotic dispersion model

Spatial moments describe the location and shape of the solute plume; that is, the position of the centroid and the spreading around the centroid, and these moments are useful in describing the transport process of non-reactive and reactive solute

Table 1 | Input parameters for the Borden Experiment

Parameter	Injected plume size	Mean pore velocity	D_0	R	C_A
Value	4.6 m × 5.6 m	0.091 m/day	0.0 $\mathrm{m^2/day}$	1	20 day

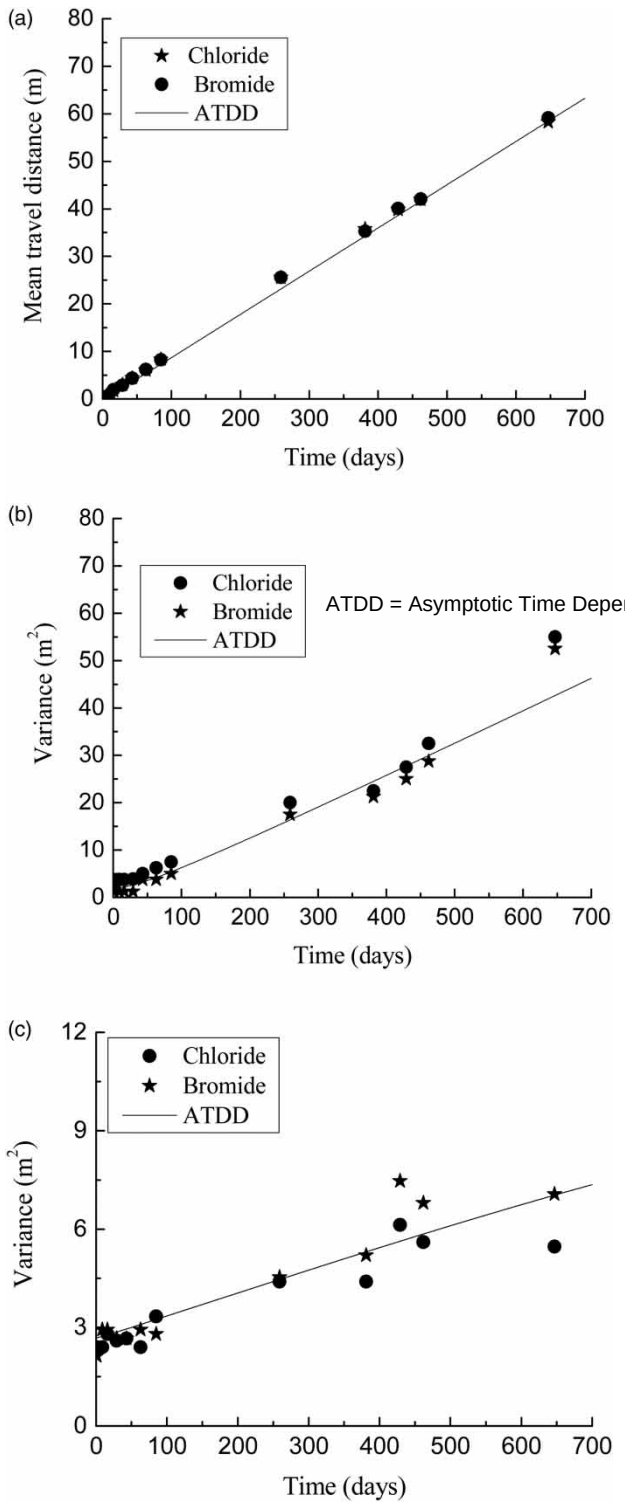

ATDD = Asymptotic Time Dependent Diffusion Coefficients

Figure 2 | (a) Simulated mean travel distance for actual experimental data of bromide and chloride chemicals from Freyberg (1986). (b) Simulated second longitudinal spatial moment for actual experiment data of bromide and chloride chemicals from Freyberg (1986). (c) Simulated transverse variance for actual experiment data of bromide and chloride chemicals from Freyberg (1986).

Zie dus artikel Freyberg

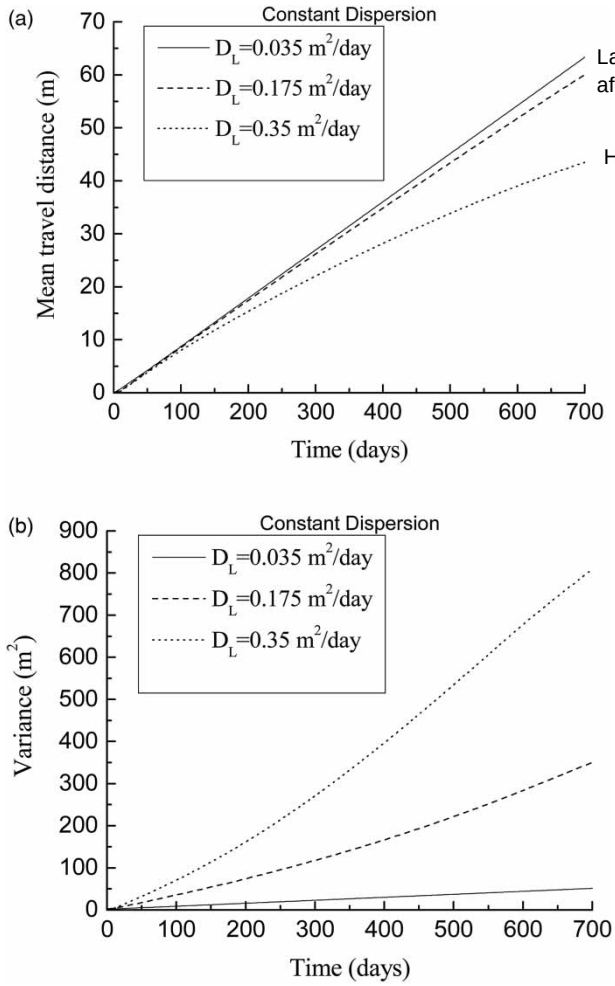

Lage DL => lineaire toename in de tijd van de gemiddelde afgelegde afstand!

Hoge DL => niet-lineaire toename van de reistijd!

Figure 3 | (a) Behavior of mean travel distance for different values of dispersion coefficient. (b) Behavior of second longitudinal spatial moments for different values of dispersion coefficient.

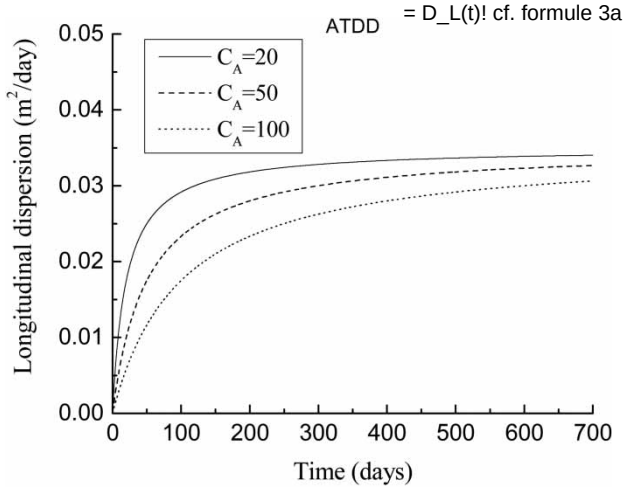

= D_L(t)! cf. formule 3a

D_L(t) = D_0 + 0.1*D * t/(t + C_A)

LAgere C_A => hogere D_L(t) waarden!

Figure 4 | Behavior of longitudinal dispersion coefficient for different values of asymptotic time-dependent coefficients.

LTDD = Linear time Dependent => formule (2a)

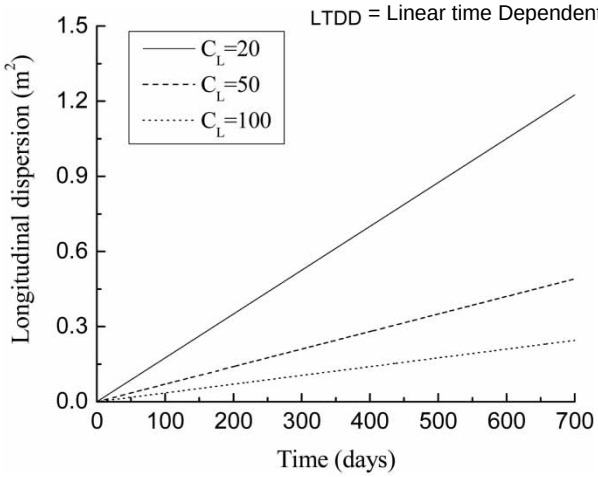

Figure 5 | Behavior of longitudinal dispersion coefficient for different values of linear time-dependent coefficients.

ATDD

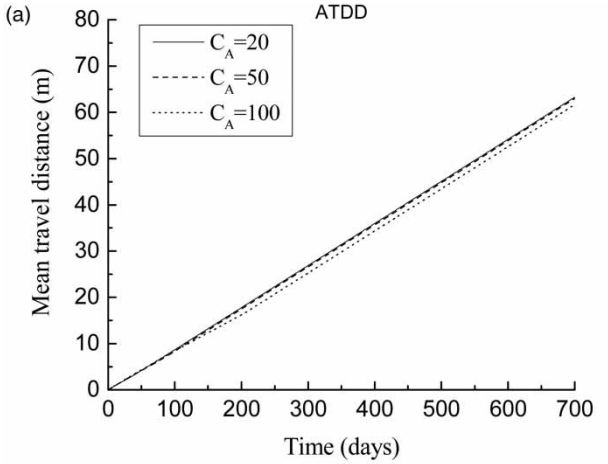

Dus wil zeggen dat verschillende waarden van de de tijdsafhankelijke asymptotische coefficient C_A weinig invloed heeft op de gemiddelde afgelegde afstand (1e moment)

D_L(t) = D_0 + 0.1*D * t/(t + C_A)

ATDD

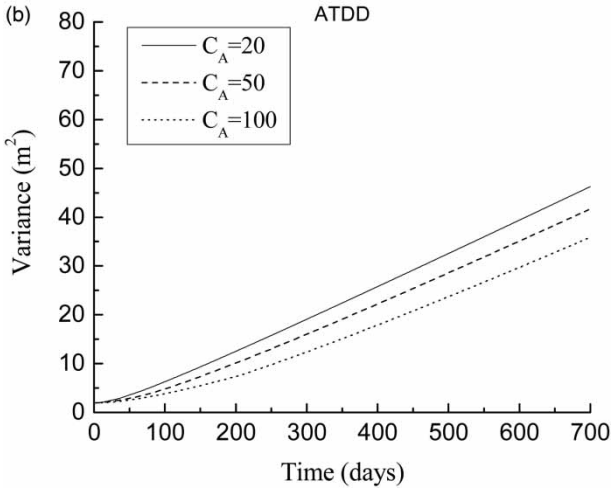

Wel een invloed op de spreiding van de pluim dus: Lagere C_A => meer spreiding! Logisch als je kijkt naar Figuur 4!

Figure 6 | (a) Behavior of mean travel distance for different values of asymptotic time-dependent coefficient. (b) Behavior of second longitudinal spatial moments for different values of asymptotic time-dependent coefficient.

through porous media. The first and second spatial moments are given, respectively, by (Deng *et al.* 1993):

$$X_i = \left(\frac{1}{M}\right) \int_{R^2} n x_i C \, dx \tag{7a}$$

$$X_{ii} = \left(\frac{1}{M}\right) \int_{R^2} n x_i^2 C \, dx - X_i^2 \tag{7b}$$

$$M = \int_{R^2} n \, c \, dx \tag{7c}$$

where M is the mass of solute, n is the porosity of the porous media, and X_i is the i^{th} moment in x coordinate direction.

The numerical model with dispersion coefficient as an asymptotic function of time is first applied for the simulation of spatial moments for two-dimensional non-reactive transport at the Borden aquifer (Freyberg 1986). The initial and boundary

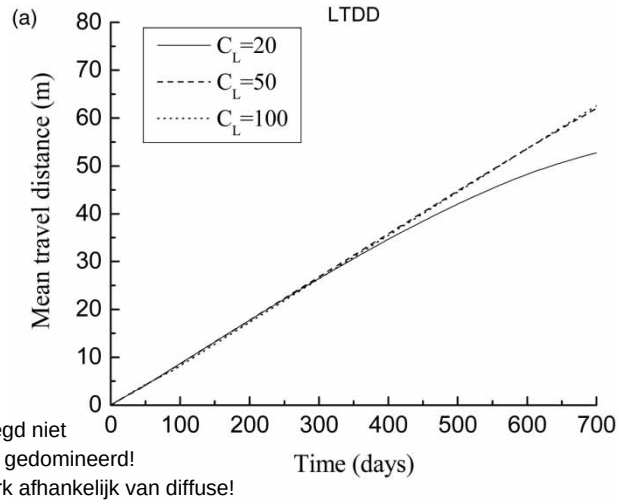

Ook voor de Lineaire tijdsafhankelijke diffusiecoeff heeft de waarden van C_L (zie formule 2a) weinig invloed op de gemiddelde afgelegde afstand

D_L = D*t/C_L + D_0

Eigen opmerking: LOGISCH dat afstand afgelegd niet sterk afhangt van diffusie, want dit is convectie gedomineerd! Spreiding van de pluim daarentegen is wel sterk afhankelijk van diffuse!

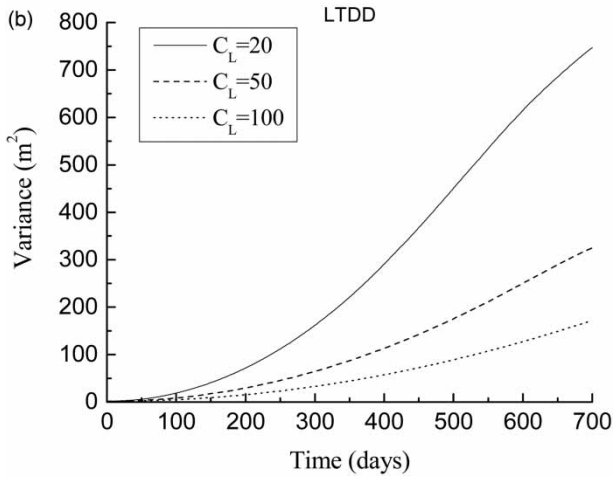

Hoe kleiner CL, hoe groter de spreiding van de pluim

Figure 7 | (a) Behavior of mean travel distance for different values of linear time-dependent coefficient. (b) Behavior of second longitudinal spatial moments for different values of linear time-dependent coefficient.

conditions are given below:

$$C(x, y, 0) = C_0 \text{ for } 10\,\text{m} \le x \le 14.6\,\text{m} \quad \text{and} \quad 4.2\,\text{m} \le y \le 9.8\,\text{m} \qquad \text{Initiële} \tag{8a}$$

$$\left.\frac{\partial C(x, y, t)}{\partial x}\right|_{x=0} = \left.\frac{\partial C(x, y, t)}{\partial x}\right|_{x=120\,\text{m}} = 0; \quad \text{and} \quad \left.\frac{\partial C(x, y, t)}{\partial y}\right|_{y=0} = \left.\frac{\partial C(x, y, t)}{\partial y}\right|_{y=14\,\text{m}} = 0 \qquad \text{Allemaal Neumann Randvoorwaarden} \tag{8b}$$

where C_0 is the initial source concentration. The input parameters used are shown in Table 1.

Figure 2(a) shows that the simulated results for the mean travel distance match very well with the observed values. As expected, for ideal transport, the mean travel distance increases linearly with time. Similarly, the simulated results of the second longitudinal and transverse moments match well with the experimental data (Figure 2(b)). Figure 2(c) represents the simulation of transverse variance of experimental field data.

Figure 3(a) and 3(b) show the behavior of mean travel distance and second spatial moment; that is, the variance of solute in the presence of different values of constant dispersion coefficient. In the presence of a smaller value of dispersion coefficient ($D_L = 0.035$ and $0.175\ m^2/day$), the mean travel distance of the solute plume increases linearly with an increase in travel time. However, in the case of the higher value of dispersion coefficient ($D_L = 0.35\ m^2/day$), the mean travel distance of a solute

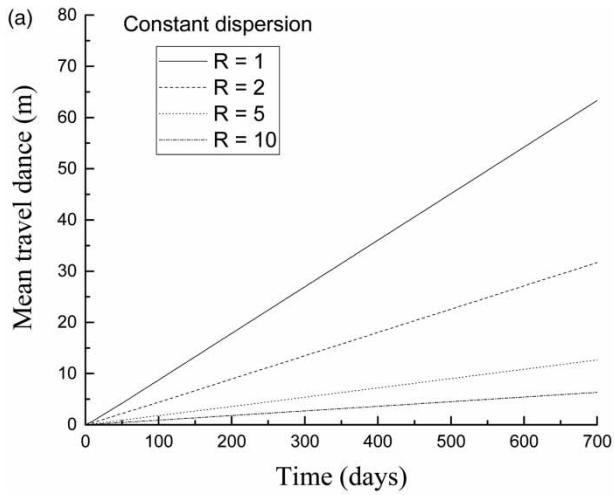

Logisch: hogere R => meer adsorptie => minder ver meereizen met de pluim!

MT bodem: R = 1 + \rho_b*K_d/eta

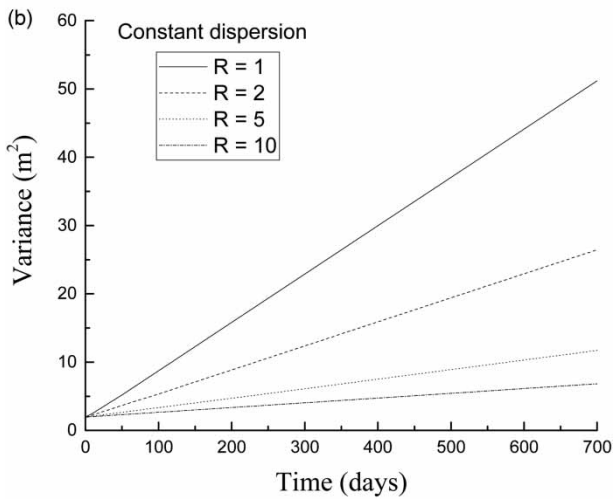

Ook variantie neemt dus af bij meer retaradatie!

Figure 8 | (a) Behavior of mean travel distance for different values of retardation coefficient. (b) Behavior of variance for different values of retardation coefficient.

plume increase non-linearly during higher transport time. The behavior of the second spatial moment is increasing non-linearly with the increase in transport time, as shown in Figure 3(b).

Figure 4 shows the variation of the longitudinal dispersion coefficient in the presence of different values of asymptotic constants. The behavior of the longitudinal dispersion coefficient increases non-linearly during short transport time while its value remains constant for higher transport time. It is also shown that the magnitude of the dispersion coefficient is higher for smaller values of asymptotic constant. However, a larger value of the asymptotic constant leads to reduction of the magnitude of the dispersion coefficient.

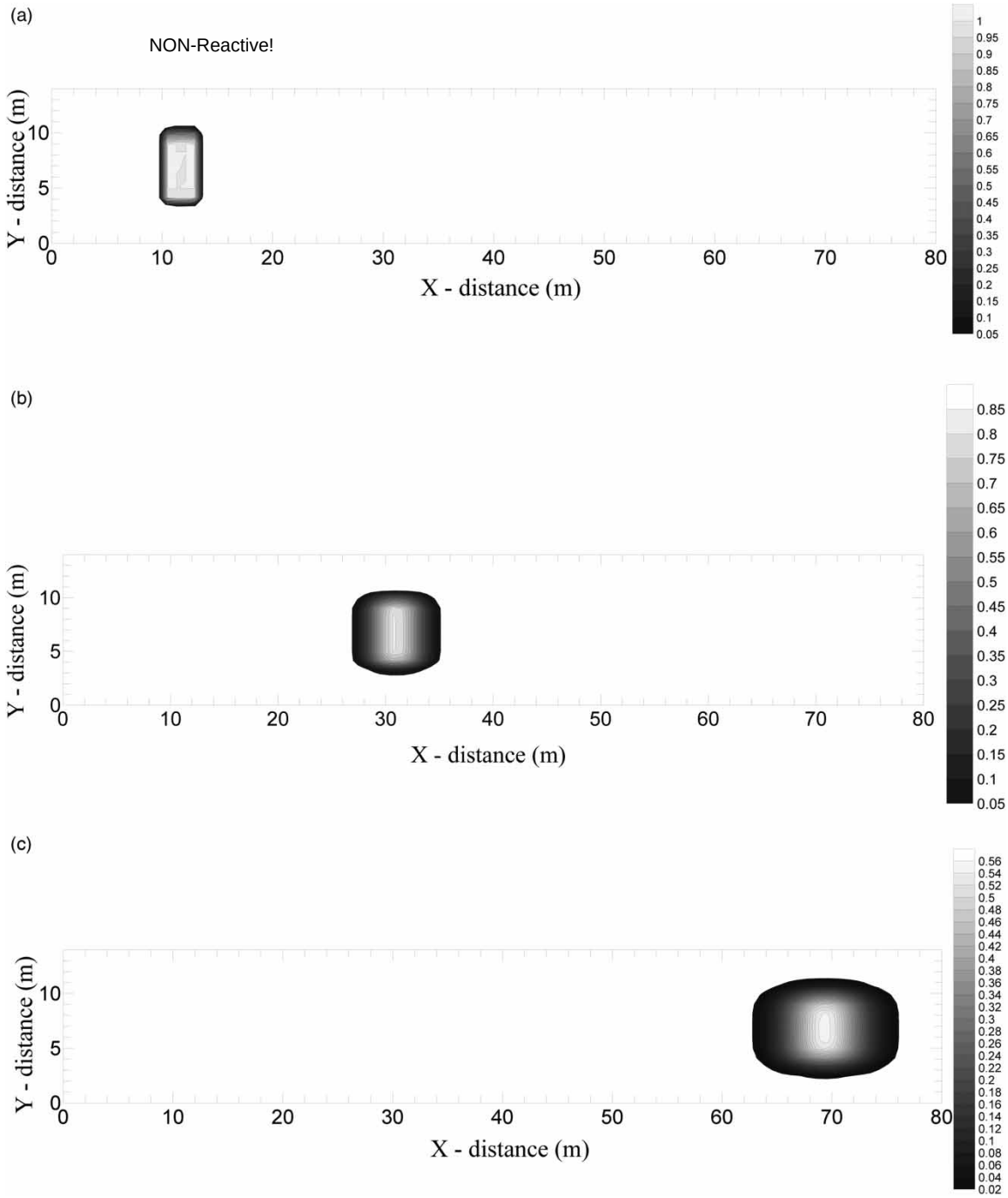

Figure 9 | (a) Initial solute concentration contour at $t = 0$ with $\alpha_L = 0.05$ m and $\alpha_T = 0.005$ m. (b) Solute concentration contour after t = 200 days with $\alpha_L = 0.05$ m and $\alpha_T = 0.005$ m. (c) Solute concentration contour after t = 600 days with $\alpha_L = 0.05$ m and $\alpha_T = 0.005$ m.

Effect of linear and asymptotic time-dependent dispersion coefficient

Figure 5 shows the variation of the longitudinal dispersion coefficient in the presence of different values of linear constants. The behavior of the longitudinal dispersion coefficient increases linearly with an increase in time in the presence of a linear constant. It is also shown that the magnitude of the dispersion coefficient is higher for smaller values of linear constant. However, a more considerable value of the linear constant leads to reduction of the magnitude of the dispersion coefficient.

Figure 6(a) shows the variation of mean travel distance in the presence of different values of asymptotic constants. The behaviour of mean travel distance increases linearly with an increase in transport time. It is also seen that the magnitude of mean travel distance remains the same in the presence of different values of the asymptotic constant. It is also shown that the magnitude of the dispersion coefficient is higher for smaller values of asymptotic constant. However, the larger value of the asymptotic constant leads to reduction of the magnitude of the dispersion coefficient. Figure 6(b) shows the behaviour of second spatial moments; that is, the variance of solute plume for different values of asymptotic constants. The higher value of asymptotic constants leads to reduce the variance; that is, spreading of the solute plume.

Figure 7(a) shows the variation of mean travel distance in the presence of different values of constants for linear time-dependent dispersion coefficients. The behaviour of mean travel distance increases linearly with an increase in transport time. It is also seen that the magnitude of mean travel distance remains the same in the presence of different values of asymptotic constant during early transport time. However, the magnitude of mean travel distance decreases non-linearly for the smaller value of constant during large transport time. But, the behaviour of variance; that is, second spatial moments, is decreasing with the increase of linear constant, as shown in Figure 7(b). Behaviour of variance is non-linear during early transport time but increases at higher transport time.

Effect of retardation factor

Figure 8(a) and 8(b) show the behavior of mean travel distance and variance of solute plume for different values of retardation coefficients. The value of the retardation coefficient equal to 1 represents the non-reactive solute plume, and the result shows that the magnitude of mean travel distance increases linearly with an increase in transport time, as shown in Figure 9(a). Values of retardation coefficients equal to 2, 5, and 10 show that solute plume is reactive. It means some of the restive solutes

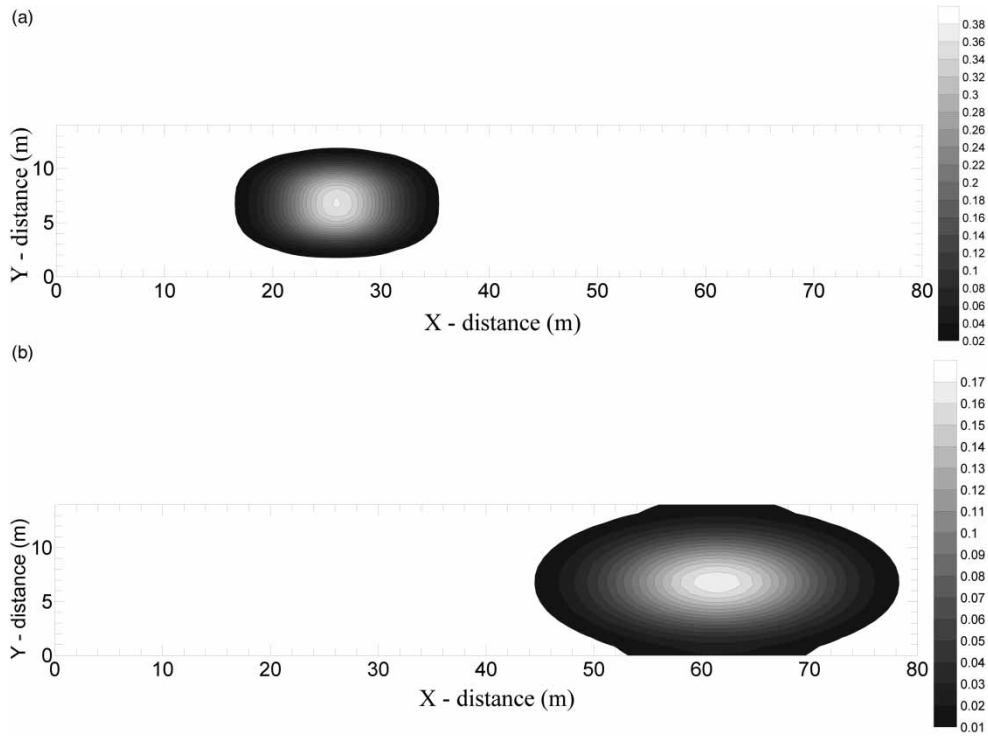

Figure 10 | (a) Solute concentration contour after t = 200 days with $\alpha_L = 0.5$ m and $\alpha_T = 0.05$ m. (b) Solute concentration contour after t = 600 days with $\alpha_L = 0.5$ m and $\alpha_T = 0.05$ m.

are adsorbed with a solid particle of soil media. Hence, higher values of retardation coefficients lead to reduction in the magnitude of mean travel distance with the increase of transport time. Similarly, the behavior of variance of the solute plume is shown in Figure 8(b). In this case, also, the magnitude of variance is decreasing for the higher value of retardation coefficients.

CONTOUR PLOTS FOR MOVEMENT OF SOLUTE PLUME

Non-reactive solute

This section describes the behavior of movement of the solute plume in the form of a contour plot in two-dimensional porous media. Figure 9(a) shows the initial location of the solute plume in the two-dimensional porous media. The value of transport parameters; that is, pore water velocity, $v = 0.1$ m/day and longitudinal dispersivity $\alpha_L = 0.05$ m, and transverse dispersivity $\alpha_T = 0.005$ m, is used during the simulation of the results. Figure 9(b) and 9(c) show the contour plots of the solute plume at

Waarom gebruik van alpha? Zijn dit nu dus opeens constante waarden van de Diffusiecoefficiënten?

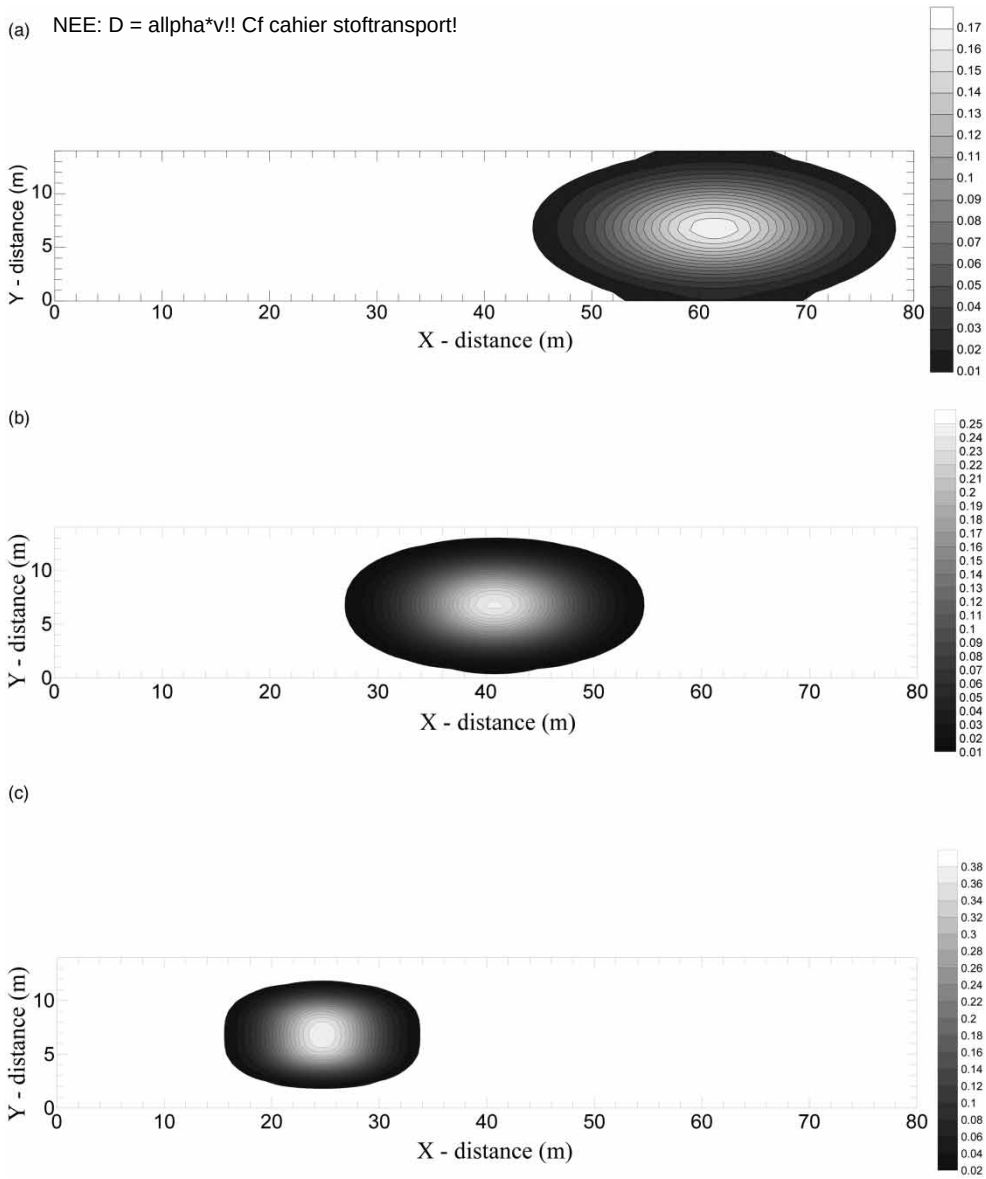

Figure 11 | (a) Solute concentration contour after t=700 days with retardation factor R = 1, α_L = .5 m and $\alpha_T = 0.05$ m. (b) Solute concentration contour after t = 700 days with retardation factor R = 2, $\alpha_L = 0.5$ m and $\alpha_T = 0.05$ m. (c) Solute concentration contour after t = 700 days with retardation factor R = 5, $\alpha_L = 0.5$ m and $\alpha_T = 0.05$ m.

Figure 12 | Experimental setup of solute transport through the physical aquifer in the lab.

transport times of 200 days and 600 days, respectively. These results show that the solute plume is moving in the flow direction, and it is also spreading in both longitudinal and transverse directions.

Higher values of longitudinal and transverse dispersivity equal to 0.5 m and 0.05 m are used for predicting the results of the movement of the solute plume. Results of various contour plots of the solute plume at transport time of 200 days and 600 days are shown in Figure 10(a) and 10(b). These results show that the spreading of the solute plume is more in case of the higher value of dispersivity as compared to a smaller value of dispersivity.

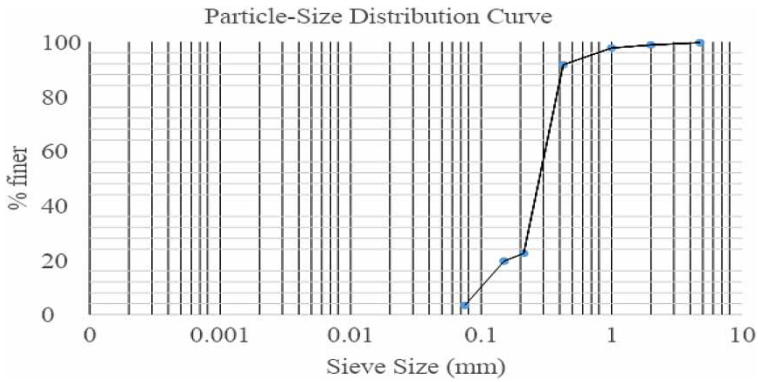

Figure 13 | Grain size distribution curve for soil.

Table 2 | Characteristics and particle size diameter of the soil

Particle size diameter (corresponds to % finer)	Size (in mm)	Characteristic coefficients	Soil classification
D_{10}	0.1	$C_u = 3.1$	SP (poorly-graded sand)
D_{30}	0.24		
D_{50}	0.28	$C_c = 1.86$	
D_{60}	0.31		

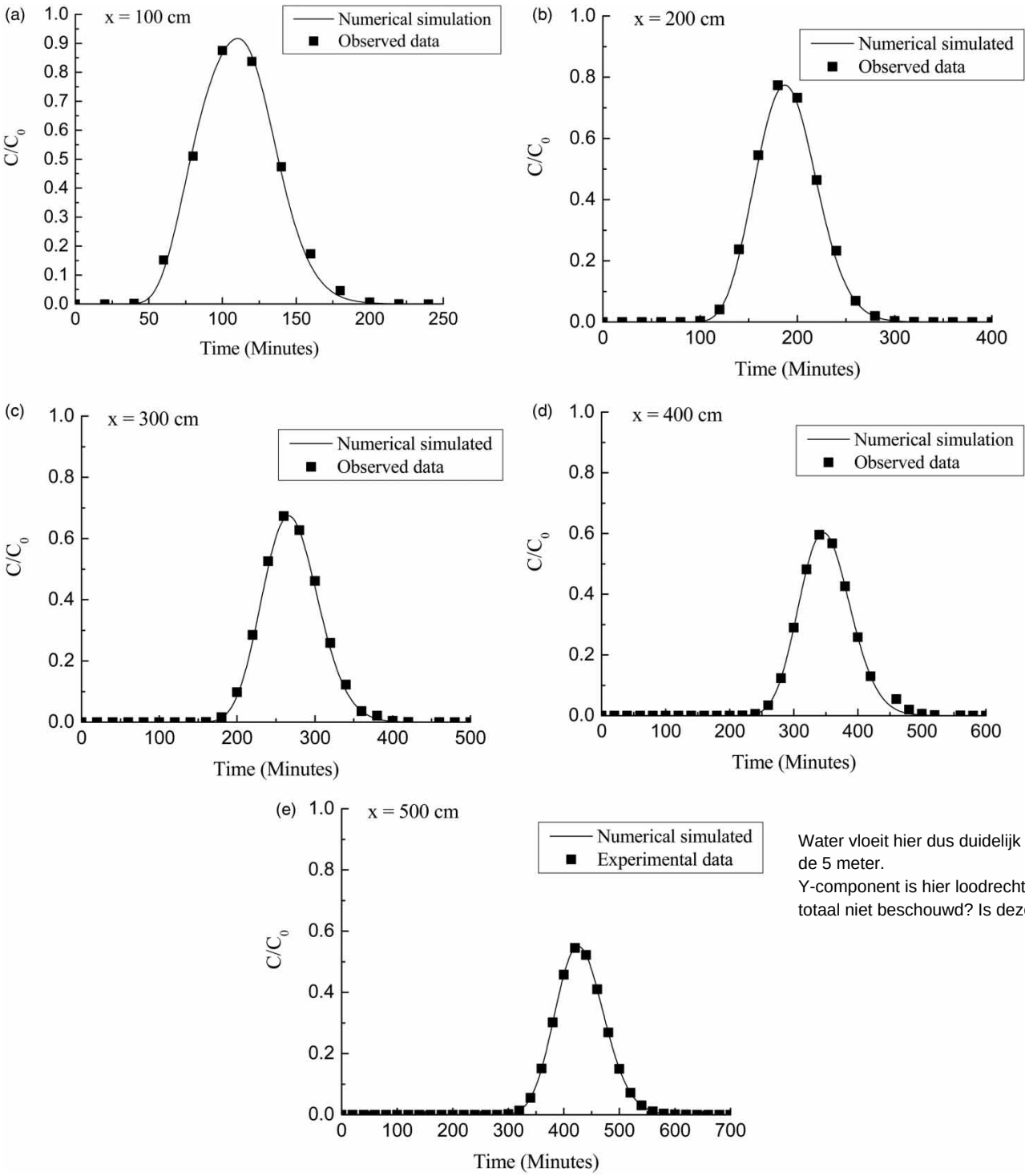

Water vloeit hier dus duidelijk HORIZONTAAL over de 5 meter.
Y-component is hier loodrecht op => wordt hier totaal niet beschouwd? Is deze weggevallen?

Figure 14 | (a) Simulation of experimental data of chloride at x = 100 cm down gradient distance in the flow direction. (b) Simulation of observed data of chloride at x = 200 cm down gradient distance in the flow direction. (c) Simulation of observed data of chloride at x = 300 cm down gradient distance in the flow direction. (d) Simulation of observed data of chloride at x = 400 cm down gradient distance in the flow direction. (e) Simulation of experimental data of chloride at x = 500 cm down gradient distance in the flow direction.

Effect of retardation coefficient

Figure 11(a)–11(c) show the results of contour plots for reactive solute plume for different values of retardation coefficient. Results show that the size of the solute plume is reduced in the presence of a higher value of retardation coefficient.

An experimental program for physical aquifer

The experimental setup consists of a 5 m × 1 m × 1 m dimensioning iron box, provided with a plexiglass material sheet of a thickness of 2 mm surrounding the lateral boundary (Figure 12). The bottom surface is provided with waterproof plywood sealed with multipurpose sealant to prevent leakage during the experiment. The iron box is painted with galvanized paint to prevent rusting and weathering effects. The inlet and outlet ends of the tank model were provided with hollow PVC pipes of diameter 2.54 cm and are sealed with a sealant material around the pipe peripherals. For investigating the tracer transport, the length of each pipe under investigation was prepared at 0.2 m, and perforations were provided at the pipe surface by the drilling machine for a full depth. The basement of the pipe was sealed to restrict the flow, and the pipe was covered with thin, clean white clothes for making the entrance of water and tracer particles into the pipes. In the homogeneous sandy porous medium, these pipes were inserted at regular intervals of 0.2 m along the transverse direction with a centrally located pipe at a distance of 0.5 m throughout the length of the porous media. The longitudinal interval between the pipes was kept at 0.5 m. The pipes were also inserted vertically at a depth interval of 0.05 m and 0.1 m from the topsoil surface to monitor the flow depth-wise.

The porous material was obtained from excavating the soil available at the site-location to a depth of about 5 m from the top surface and was filled up to the depth of 30 cm from the bottom of the tank. The soil was excavated to conduct the experimental studies on a porous material having representative physiochemical properties of agricultural fields. This type of study will be useful to understand the problem of the transport of fertilizers and salts in the subsurface so that the risk of groundwater quality can be minimized. The physical properties of the soil material were obtained by performing experiments in the geotechnical lab. During the experiments, the test material was sieved using standard mechanical sieves to obtain the particle size distribution of the soil material. The graphical plot on a semi-logarithmic scale, as shown in Figure 13, represents the variation of grain sizes present in the soil sample, in mm, with respect to the percentage finer by weight. The material characteristic properties were studied by determining the value of the coefficient of uniformity (C_U) and coefficient of curvature (C_C) of the test sample. Table 2 shows the characteristic values of the coefficients along with the median grain sizes. The soil was classified using the Indian standard soil classification system, and the material was found to be poorly graded sandy soil, falling under the SP category.

The layering of sand in the tank model was done by compacting the sand in three equivalent layers at optimum moisture content to a depth of about 2 feet (0.6 m) from the invert level. The packaging of the sandy layers is done at a maximum dry density so as to minimize the voids present in the porous medium. The bulk density and dry density of the sample as determined by the sand replacement method were found to be 1.85 g/cm^3 and 1.54 g/cm^3, respectively. The pore water velocity is estimated to be 0.86 cm/min. The hydraulic conductivity of 1.12×10^{-3} cm/min was measured by using the falling head method. The porosity of the medium was determined to be 0.39.

Zelf snelle check via darcy: v = -K/eta*dh/dx = 1.12e-3 cm/min*1/0.39*?? => de Hydraulische gradiënt ontbreekt hier...

SIMULATION OF EXPERIMENTAL DATA OF BREAKTHROUGH CURVES

The numerical model has been used to simulate observed breakthrough curves for non-reactive as chloride and reactive solute as fluoride through porous media. Experimental data of observed breakthrough curves have been predicted at 100 cm, 200 cm, 300 cm, 400 cm, and 500 cm down gradient direction in the flow direction.

Table 3 | Estimation of R^2, RMSE, and NSE for simulation of breakthrough curves of chloride

Distance (cm)	R^2 Niet-lineair => geen R^2	RMSE	NSE
100	0.9964	0.0238	0.9946
200	0.9992	0.0154	0.9970
300	0.9988	0.0147	0.9961
400	0.9981	0.0107	0.9973
500	0.9997	0.0027	0.9996

Op welke y werden deze bepaald? of aggregeren we nu over y?

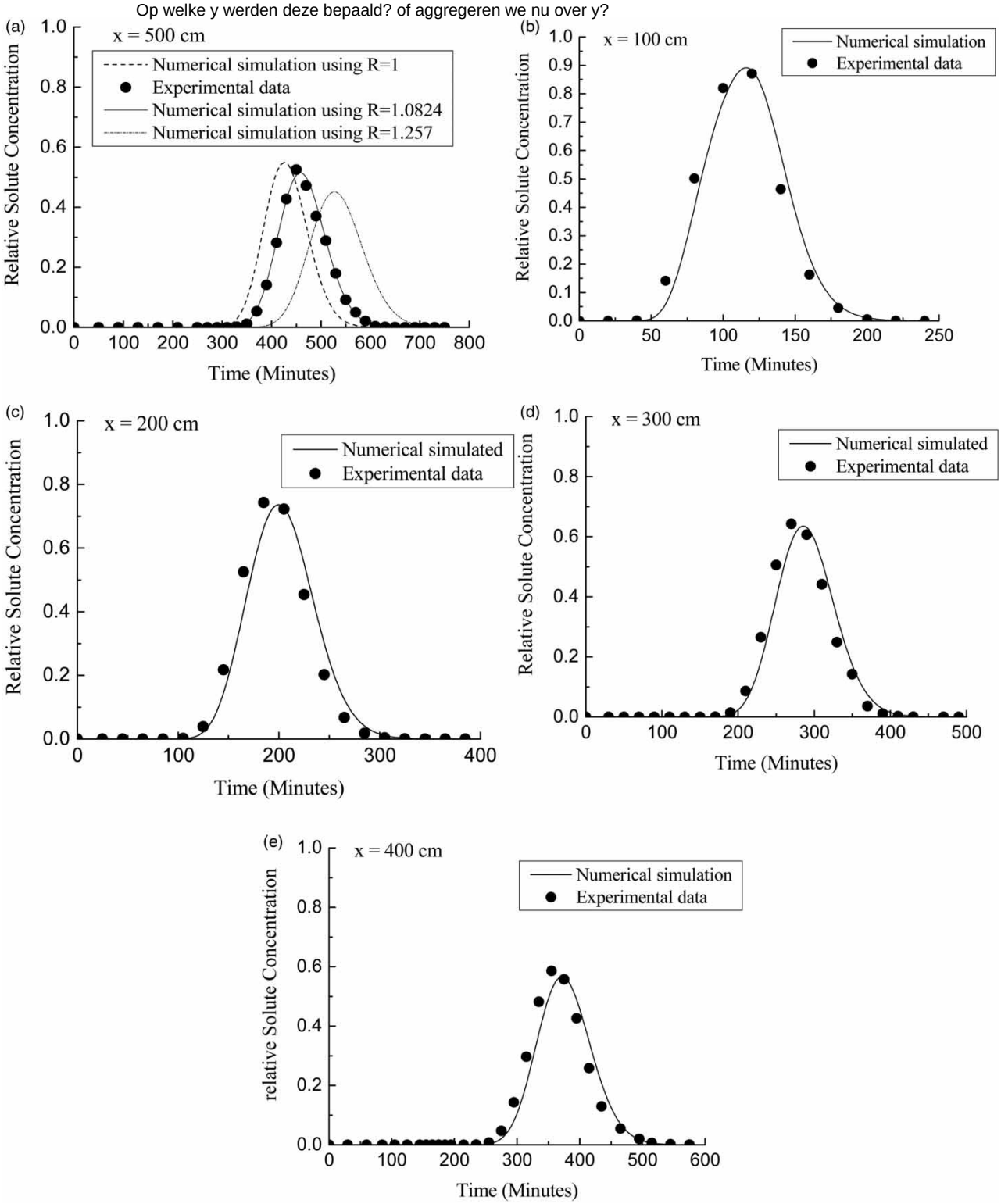

Figure 15 | (a) Simulation of observed data of fluoride at x = 500 cm down gradient distance in the flow direction. (b) Simulation of observed data of fluoride at x = 100 cm down gradient distance in the flow direction. (c) Simulation of observed data of fluoride at x = 200 cm down gradient distance in the flow direction. (d) Simulation of observed data of fluoride at x = 300 cm down gradient distance in the flow direction. (e) Simulation of observed data of fluoride at x = 400 cm down gradient distance in the flow direction.

Table 4 | Estimation of R^2, RMSE and NSE for simulation of breakthrough curves for fluoride

Distance (cm)	R^2	RMSE	NSE
100	0.9423	0.0744	0.9407
200	0.9254	0.0741	0.9249
300	0.9304	0.0603	0.9303
400	0.8985	0.0650	0.8959
500	0.9933	0.0154	0.9921

Experimentally observed data of chloride

Experimental data of observed breakthrough curves are shown for discharge flux rate equal to 1.248 cm/min and pore water velocity equal to 3.2 cm/min. During experiments, constant flux was maintained by keeping the constant head at the inlet and outlet of the tank and it was verified by maintaining a constant flow at the outlet ensuring no leakage in the tank. All the breakthrough curves are simulated well predicted in the flow direction and are shown in Figure 14(a)–14(e). From the above analysis, it is shown that the spreading and peak of breakthrough curves are higher for smaller distances, and the magnitude of the peak of breakthrough curves is reduced at a large travel distance in the flow direction. Estimation of the correlation coefficient, root mean square error, and NSE during simulation of observed breakthrough curves at a different distance in the flow direction is shown in Table 3.

Experimental data of fluoride

Figure 15(a) shows the simulation of observed breakthrough curves for fluoride predicted at 500 cm down gradient distance in the flow direction. Input parameters; that is, pore water velocity $v = 3.2$ cm, longitudinal hydrodynamic dispersion coefficient $D_L = 8\ cm^2/min$, and transverse dispersion coefficient $D_T = 0.8\ cm^2/min$, are used during simulation. Afterward, different values of retardation coefficient, R = 1, 1.0824a, and 1.257, are used. It is seen that the value of the retardation coefficient equal to 1.0824 gives the best simulation of the observed breakthrough curve. This value of retardation coefficient equal to 1.0824 is used to simulate the observed breakthrough curves at 100 cm, 200 cm, 300 cm, and 400 cm down gradient distance in the flow direction. Estimation of the correlation coefficient, root mean square error, and NSE during simulation of observed breakthrough curves at a different distance in the flow direction is shown in Table 4.

CONCLUSION

Based on the above study, the following conclusions are mentioned below:

1. Experimental data of spatial moments for bromide and chloride chemicals (Freyberg 1986) are simulated well using an asymptotic time-dependent dispersion model. The higher value of dispersion coefficient leads to a decrease in the value of mean travel distance and increases the value of variance during large transport time. The behaviour of variance is non-linear during small transport time in the presence of a higher value of dispersion coefficient.
2. Variation of longitudinal dispersion coefficients has been predicted in the presence of linear and asymptotic constants. The value of the dispersion coefficient decreases with an increase in the values of both linear and asymptotic constants. However, the behaviour of the dispersion coefficient is non-linear during early transport time, and its magnitude remains constant for large transport time. It is also shown that magnitude of mean travel distance and variance of the solute plume is decreasing with an increase in the value retardation coefficient. It means that the sorption of reactive solute retards the movement of the solute plume in the flow direction.
3. Experimentally observed breakthrough curves of chloride and fluoride solutes were predicted and simulated using a numerical model. Thus, estimated parameters such as a dispersion coefficient equal to $8\ cm^2/min$ and retardation factor equal to 1.0824 are found through numerical simulation of observed data of breakthrough curves. The movement of conservative chloride solute within the porous medium is faster than reactive fluoride due to sorption with soil media. Finally, this study shall be useful to understand the problem of the transport of fertilizers and salts in the subsurface so that the risk to groundwater quality can be minimized.

CONFLICT OF INTEREST

The authors declared that there is no conflict of interest.

DATA AVAILABILITY STATEMENT

All relevant data are included in the paper or its Supplementary Information.

REFERENCES

Al Kuisi, M., Al-Qinna, M., Margane, A. & Aljazzar, T. 2009 Spatial assessment of salinity and nitrate pollution in Amman Zarqa Basin: a case study. *Environmental Earth Sciences* **59** (1), 117–129.

Anderson, M. P. & Cherry, J. A. 1979 Using models to simulate the movement of contaminants through groundwater flow systems. *Critical Reviews in Environmental Science and Technology* **9** (2), 97–156.

Apiratikul, R. 2020 Application of analytical solution of advection-dispersion-reaction model to predict the breakthrough curve and mass transfer zone for the biosorption of heavy metal ion in a fixed bed column. *Process Safety and Environmental Protection* **137**, 58–65.

Aral, M. M. & Liao, B. 1996 Analytical solutions for two-dimensional transport equation with time-dependent dispersion coefficients. *Journal of Hydrologic Engineering* **1** (1), 20–32.

Aris, R. 1956 On the dispersion of a solute in a fluid flowing through a tube. *Proceedings of the Royal Society of London. Series A. Mathematical and Physical Sciences* **235** (1200), 67–77.

Barry, D. A. & Sposito, G. 1989 Analytical solution of a convection-dispersion model with time-dependent transport coefficients. *Water Resources Research* **25** (12), 2407–2416.

Basha, H. A. & El-Habel, F. S. 1993 Analytical solution of the one-dimensional time-dependent transport equation. *Water Resources Research* **29** (9), 3209–3214.

Batu, V. 1989 A generalized two-dimensional analytical solution for hydrodynamic dispersion in bounded media with the first-type boundary condition at the source. *Water Resources Research* **25** (6), 1125–1132.

Batu, V. 1993 A generalized two-dimensional analytical solute transport model in bounded media for flux-type finite multiple sources. *Water Resources Research* **29** (8), 2881–2892.

Belhachemi, M. & Addoun, F. 2011 Comparative adsorption isotherms and modelling of methylene blue onto activated carbons. *Applied Water Science* **1** (3–4), 111–117.

Chiogna, G., Eberhardt, C., Grathwohl, P., Cirpka, O. A. & Rolle, M. 2010 Evidence of compound-dependent hydrodynamic and mechanical transverse dispersion by multitracer laboratory experiments. *Environmental Science and Technology* **44** (2), 688–693.

Corey, J. C., Hawkins, R. H., Overman, R. F. & Green, R. E. 1970 Miscible displacement measurements within laboratory columns using the gamma-photoneutron method. *Soil Science Society of America Journal* **34** (6), 854–858.

Dehghan, M. 2004 Numerical solution of the three-dimensional advection–diffusion equation. *Applied Mathematics and Computation* **150** (1), 5–19.

Deng, F. W., Cushman, J. H. & Delleur, J. W. 1993 A fast Fourier transform stochastic analysis of the contaminant transport problem. *Water Resources Research* **29** (9), 3241–3247.

Farrell, D. A., Woodbury, A. D. & Sudicky, E. A. 1994 The 1978 Borden tracer experiment: analysis of the spatial moments. *Water Resources Research* **30** (11), 3213–3223.

Fenske, P. R. 1979 Time-dependent sorption on geological materials. *Journal of Hydrology* **43** (1–4), 415–425.

Freeze, R. A. & Cherry, J. A. 1979 *Groundwater (No. 629.1 F7)*.

Freyberg, D. L. 1986 A natural gradient experiment on solute transport in a sand aquifer: 2. Spatial moments and the advection and dispersion of non-reactive tracers. *Water Resources Research* **22** (13), 2031–2046.

Fried, J. J. 1975 *Groundwater Pollution*. Elsevier Applied Science, New York, NY.

Gao, G., Zhan, H., Feng, S., Fu, B., Ma, Y. & Huang, G. 2010 A new mobile-immobile model for reactive solute transport with scale-dependent dispersion. *Water Resources Research* **46** (8), 1–16.

Gelhar, L. W. & Axness, C. L. 1983 Three-dimensional stochastic analysis of macrodispersion in aquifers. *Water Resources Research* **19** (1), 161–180.

Gelhar, L. W., Gutjahr, A. L. & Naff, R. L. 1979 Stochastic analysis of macrodispersion in a stratified aquifer. *Water Resources Research* **15** (6), 1387–1397.

Goltz, M. N. & Roberts, P. V. 1987 Using the method of moments to analyze three-dimensional diffusion-limited solute transport from temporal and spatial perspectives. *Water Resources Research* **23** (8), 1575–1585.

Huang, K., Toride, N. & Van Genuchten, M. T. 1995 Experimental investigation of solute transport in large, homogeneous and heterogeneous, saturated soil columns. *Transport in Porous Media* **18** (3), 283–302.

James, A. I. & Jawitz, J. W. 2007 Modeling two-dimensional reactive transport using a Godunov-mixed finite element method. *Journal of Hydrology* **338** (1–2), 28–41.

Joshi, N., Ojha, C. S. P. & Sharma, P. K. 2012 A non-equilibrium model for reactive contaminant transport through fractured porous media: model development and semi analytical solution. *Water Resources Research* **48**, W10511. doi:10.1029/2011WR011621.

Knorr, B., Maloszewski, P., Krämer, F. & Stumpp, C. 2016 Diffusive mass exchange of non-reactive substances in dual-porosity porous systems–column experiments under saturated conditions. *Hydrological Processes* **30** (6), 914–926. doi.org/10.1002/hyp.10620.

Latinopoulos, P., Tolikas, D. & Mylopoulos, Y. 1988 Analytical solutions for two-dimensional chemical transport in aquifers. *Journal of Hydrology* **98** (1–2), 11–19.

Leij, F. J., Skaggs, T. H. & van Genuchten, M. T. 1991 Analytical solutions for solute transport in three-dimensional semi-infinite porous media. *Water Resources Research* **27** (10), 2719–2733.

Leij, F. J., Toride, N. & Van Genuchten, M. T. 1993 Analytical solutions for non-equilibrium solute transport in three-dimensional porous media. *Journal of Hydrology* **151** (2–4), 193–228.

Leij, F. J., Toride, N., Field, M. S. & Sciortino, A. 2012 Solute transport in dual-permeability porous media. *Water Resources Research* **48** (4), 1–13.

Levy, M. & Berkowitz, B. 2003 Measurement and analysis of non-Fickian dispersion in heterogeneous porous media. *Journal of Contaminant Hydrology* **64** (3–4), 203–226.

Marinoschi, G., Jaekel, U. & Vereecken, H. 1999 Analytical solutions of three-dimensional convection-dispersion problems with time dependent coefficients. *ZAMM-Journal of Applied Mathematics and Mechanics/Zeitschrift für Angewandte Mathematik und Mechanik: Applied Mathematics and Mechanics* **79** (6), 411–421.

Masciopinto, C. & Passarella, G. 2018 Mass-transfer impact on solute mobility in porous media: a new mobile-immobile model. *Journal of Contaminant Hydrology* **215**, 21–28.

Neville, C. J., Ibaraki, M. & Sudicky, E. A. 2000 Solute transport with multiprocess non-equilibrium: a semi-analytical solution approach. *Journal of Contaminant Hydrology* **44** (2), 141–159.

Ogata, A. & Banks, R. B. 1961 *A Solution of the Differential Equation of Longitudinal Dispersion in Porous Media: Fluid Movement in Earth Materials*. US Government Printing Office, Washington, DC.

Pickens, J. F. & Grisak, G. E. 1981 Modeling of scale-dependent dispersion in hydrogeologic systems. *Water Resources Research* **17** (6), 1701–1711.

Selvadurai, A. P. S. 2004 On the advective-diffusive transport in porous media in the presence of time-dependent velocities. *Geophysical Research Letters* **31** (13), 1–5.

Serrano, S. E. 1995 Forecasting scale-dependent dispersion from spills in heterogeneous aquifers. *Journal of Hydrology* **169** (1–4), 151–169.

Sharma, P. K., Ojha, C. S. P., Swami, D., Joshi, N. & Shukla, S. K. 2015 Semi-analytical solutions of multiprocessing non-equilibrium transport equations with linear and exponential distance-dependent dispersivity. *Water Resources Management* **29** (14), 5255–5273.

Šimůnek, J. & Suarez, D. L. 1994 Two-dimensional transport model for variably saturated porous media with major ion chemistry. *Water Resources Research* **30** (4), 1115–1133.

Xu, T., Ye, Y., Zhang, Y. & Xie, Y. 2019 Recent advances in experimental studies of steady-state dilution and reactive mixing in saturated porous media. *Water* **11** (1), 3. doi:10.3390/w11010003.

Yates, S. R. 1990 An analytical solution for one-dimensional transport in heterogeneous porous media. *Water Resources Research* **26** (10), 2331–2338.

Yates, S. R. 1992 An analytical solution for one-dimensional transport in porous media with an exponential dispersion function. *Water Resources Research* **28** (8), 2149–2154.

Zoppou, C. & Knight, J. H. 1999 Analytical solution of a spatially variable coefficient advection–diffusion equation in up to three dimensions. *Applied Mathematical Modelling* **23** (9), 667–685.

First received 27 February 2021; accepted in revised form 16 August 2021. Available online 26 August 2021